山口大学教育学部研究論叢　第 71 巻　255 頁～ 267 頁　2022 年 1 月

Characterization of the Blue Protein in the Shell-Surface Pattern of the Japanese Littleneck Clam (*Ruditapes philippinarum*)

MURAKAMI Kiyofumi, OHTAWA Hiromi, TOKUDA Tomoe,
KANEBAYASHI Yasue, YASUDA Yuko, WAIZUMI Kenji

(Received September 24, 2021)

ABSTRACT

Characterization of the blue protein in the shell pattern of Japanese littleneck clam (*Ruditapes philippinarum*) was performed by purification using anion-exchange chromatography, amino acid analysis, molecular weight measurements, quantification of ferric ions, etc. Blue colored two components were found by anion exchange chromatography. The blue colored shell protein and the colorless mantle protein were found to be homologous to each other in amino acid composition; they are acidic proteins rich in aspartic acid and glutamic acid and that the isoelectric point of the blue protein was estimated as *pI*=3.96. The secondary structures of the blue protein were estimated as α-helix (28.6%), β-sheet (20.1%), and random coil (51.3%). From combination of molecular weight measurements and quantification of ferric ions, it was found that the blue protein is formed as trimer or tetramer from the monomer proteins of about 10 kDa by complexing with ferric ion. It was also found that there are two kinds of ferric ion existing states and that reducing agents decompose the blue colored trimer or tetramer into dimer or smaller units accompanying decolorization.

1. INTRODUCTION

Biomineralization is a universal phenomenon found in all living organisms from unicellular organisms to plants and animals. Among them, the biomineral with the highest biomass on the earth is calcium carbonate. Calcium ion is present in large quantity in seawater and strongly electrostatically interact with carbonate ions to form calcium carbonate. Calcium carbonate is used for support of soft body and protection from foreign enemies (Kobayashi 1996), mineral storage (Kobayashi 1996), and gravity sensing (Kondrachuk and Wiederhold 2001; Kondrachuk and Boyle 2006).

Mollusk shells are formed by calcium carbonate crystals and by insoluble organic matrix that surrounds them. In mollusks, it was known that there are many acidic amino acids from analysis of amino acid composition of the organic matrix contained in the hard tissue. Therefore, it has been considered important for the formation of the hard tissue that acidic proteins containing a large amount of acidic amino acids are negatively charged and interact with positively charged calcium ions. Furthermore, it has been pointed out that the crystal form may be controlled by the arrangement of acidic amino acids in the protein. It has been shown that water-soluble substrate proteins play a central role in the "calcite-aragonite problem" (Falini et al., 1996; Belcher et al., 1996).

Abundant groups of pigment of marine fishes and invertebrates including mollusks are broadly classified into three groups. The first group is that of porphyrins and bile pigments. The pigments with colors ranging from blue to green are known to be present in many tissues of marine fishes and mollusks, as a complex with protein. Biliverdins and related compounds are known to be present in blood serum of eel (Kochiyama et al. 1966) and family cottidae (Low and Bada 1974), muscle of ao-hirosa (*Cheilinus undulatus*) (Yamaguchi and Matsuura

Department of Science, Faculty of Education, Yamaguchi University, Yoshida 1677-1, Yamaguchi 753, Japan

1969), erythrocytes of flying fish, scales of sculpin and saury, ovary of turban shell (*Turbo sazae*) (Yamaguchi and Ogata 1978, Benedikt et al., 1988), and shell of tokobushi (*Monodonta turbinata*) (Bannister et al. 1970). Many of these pigments bind to apoproteins by covalent bonds. Molecular weights of those pigment-protein complexes have been reported as ranging from 10 kDa to 1000 kDa, by using size exclusion chromatography or gel-electrophoresis. Concerning porphyrins, protoporphyrin and uroporphyrin are observed in the shells of marine snails and bivalves (Verdes et al. 2015, Williams et al. 2016, Bonnard et al. 2020). However, the state of presence of these pigments is not clear yet.

The second group is carotenoid. Non-covalent association between carotenoid and apoprotein is common among the marine invertebrates showing a multitude of colors (blue, green, purple, red etc.) (Wade et al. 2009). Among those, crustacyanin in exoskeleton of lobsters exhibits blue color (Milicua et al. 1985, Zagalsky 1985). The chromophore is astaxanthin. The complex between astaxanthin and apoprotein forms β-crustacyanin (dimer of the complex; Mw=40kDa). Eight β-crustacyanins associate each other to form α-crustacyanin (Mw=320 kDa). The blue color develops by bathochromic shift due to the higher-order structuring (Cianci et al. 2002). Concerning molluscan shell color pigments, although polyene compounds have often been suggested to be carotenoids based on Raman spectral features (Barnard and Waal 2006, Hedegaard et al. 2006, de Oliveira et al. 2013), further investigations are expected for definitive identification (Williams 2017).

The third group is melanin. The melanin pigments are believed to be responsible for dark, tan, and even yellowish or reddish pigmentations, and are derived by the oxidation and polymerization of tyrosine or phenolic compounds. There are two forms of melanin in mollusk: eumelanin and pheomelanin. For example, eumelanin is a component of cephalopod ink (Dubey and Roulin 2014). Pheomelanin has recently been found in chiton shell-eyes (Speiser et al. 2014). It has generally been thought that tyrosinase plays an important role in melanin synthesis. The formation of an abnormal pearl with a blue shade on the surface is suggested as being caused by a tyrosinase (Miyashita and Takagi 2011). From the expression pattern of the tyrosinase genes in the mantle of different shell-color strains of Manila clam (*Ruditapes philippinarum*), it was suggested that tyrosinases might be involved in different shell-color formation (Jiang et al. 2020). On the other hand, it was recently found that many brown and black color patterns on bivalve and gastropod shells, commonly considered melanin, are not necessarily of melanic origin (Affenzeller et al. 2019). Furthermore, the most highly expressed genes encoding for tyrosinase are found in the pallial mantle, which is responsible for producing the nacreous, unpigmented layer of shell (Zhang et al. 2012). The authors suggest that the oxidation of tyrosine may be essential for shell matrix maturation.

Pigmentation in mollusk shells has also been of interest from the perspective of pattern formation. Two models have been proposed to explain the pattern formation of mollusk shells. One is the diffusion-reaction model in which diffusing morphogens play central roles (Meinhardt 1984, Meinhardt and Klingler 1987, Fowler et all. 1992, Meinhardt et al. 2003). Although substantive basis of the morphogens has not been clarified, the models can be viewed as an analogy for neural activity (Murray 2003). The other is the neural model in which the mantle neural net can encode the appropriate information required for shell growth as well as pigment deposition (Saleuddin ASM 1979, Saleuddin and Kunigelis 1984, Boettiger et al. 2009). The latter neural net model may reflect the actual situation. However, as in the case of the diffusion-reaction model, the material basis of pigmentation has not been of well understand yet.

In the previous study (Murakami and Tamura 1995), the authors found that a blue polymer (protein) was extracted as an aqueous solution from the shell of Japanese littleneck clam (*Ruditapes philippinarum*) by an aqueous acetic acid solution (Fig. 1 (A)). This protein solution has a light absorption peak at 627 nm. This experiment clarified the composition principle of the shell-surface-pattern color of the clam, as follows. The surface of the shell (periostracum) is composed of two layers; the outer layer in contact with seawater is brown or transparent color depending on the lateral position along the shell edge, the inner layer inside it is blue or white (the color of calcium carbonate), and the brown area of the outer layer and the blue area of the inner layer overlap exactly. By superimposing these colors of the two layers, five surface pattern colors of the shell appear. That is, white (transparent outer layer + white inner layer), brown (brown outer layer + white inner layer) (Fig.1 (B) upper left-hand side), green (light brown

outer layer + light blue inner layer), blue (transparent outer layer + blue inner layer) and black (dark brown outer layer + dark blue inner layer) (Fig 1 (B) lower left-hand side). It was also found that iron and aluminum are bound to this blue protein, and that the color tone of the aqueous solution changes by the addition of alkali, alcohols, surfactants or by heating. However, the detailed molecular properties of the protein and the mechanism of the color development are not clear yet.

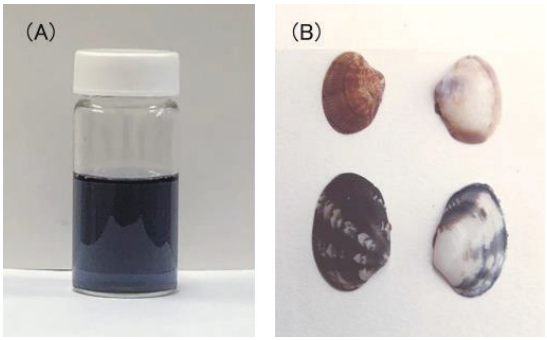

Figure 1. (A) Blue protein solution extracted from the shell of Japanese littleneck clam (*Ruditapes philippinarum*) by 0.1 moldm^{-3} aqueous acetic acid solution. (B) State of shell surface pattern before (left hand side) and after (right hand side) the acetic acid treatment. The shells on the upper side are brown colored ones, and those on the lower side are black shells.

Clarifying the properties of the blue protein, especially the cause of blue coloration, will contribute to elucidate the mechanism of the pattern formation from material basis. The purpose of this study is to characterize the blue protein that causes the surface pattern color of the shell of Japanese littleneck clam (*Ruditapes philippinarum*).

2. EXPERIMENTAL

Materials Live specimens of Japanese littleneck clam (*Ruditapes philippinarum*) have been collected on the coast of Ajisucho-Higashikiwa in yamaguchi city.

Extraction and purification of the blue protein The blue protein was extracted from the shell by immersing the outer part of the shell in a 0.1 moldm^{-3} aqueous acetic acid solution. After filtration by a filter paper and extensive dialysis against water, the protein was precipitated out by $(NH_4)_2SO_4$ at 60% saturation. The precipitate was collected by a centrifugation, and was dissolved in a large amount of 0.01 moldm^{-3} phosphate buffer (pH=7.0), and was adsorbed on an anion exchange resin (DEAE-TOYOPEARL650) column (26.4 mm×450 mm) equilibrated with the same buffer solution, and then eluted with a linear gradient of NaCl (0—1 moldm^{-3}). By collecting the blue fractions with absorbance more than 0.2, the above procedure was repeated once more. The blue fractions with absorbance more than 0.2 obtained by the second-time chromatography were dialyzed against water to remove the salt for subsequent analyses.

For comparison, the protein sample from the mantle was prepared as follows. To 44 g of the mantle tissue, 100 ml of an aqueous acetic acid solution of 1 moldm^{-3} was added, and the mixture was finely crushed using a mixer. The sample was filtered and then centrifuged at 5000 rpm for 20 min using Sakuma Model 55-1 at a low temperature. The supernatant was filtered and collected. The sample was extensively dialyzed against distilled water at low temperature for 4 days while exchanging the external solution twice a day. The subsequent purification procedures are the same as those for the blue protein from the shell.

Amino-acid analysis and estimation of isoelectric point The sample prepared as above was lyophilized and 6N hydrochloric acid was added to prepare a concentration of 0.1 mg/mL. This sample solution was degassed, sealed, and hydrolyzed in an aluminum heating block at 110 ℃ for 24 hours. After hydrolysis, hydrochloric acid was removed by spraying nitrogen gas. To the residue, 500 μl of citric acid buffer (pH=2.2) was added for amino acid analysis, dissolved, and filtered through a membrane filter. The analysis was performed with an IRIKA Automatic Amino Acid Analyzer Model A-5500. In this analysis, some of tryptophan, cysteine and cystine might not be detected because of hydrochloric acid hydrolysis under the normal condition. Isoelectric point of the blue protein was estimated by using Protein Identification and Analysis Tools on the ExPASy Server (Gasteiger et al. 2003).

Molecular weight measurements

Size exclusion chromatography (SEC) To evaluate the molecular weights under the native condition, the peak fractions A and B, that were obtained by the anion-exchange chromatography, have been subjected to size-exclusion chromatography on a Toso HPLC system with TSK3000SWxL column (7.8 mm×300 mm) in 0.1 mol dm^{-3} phosphate buffer (pH=7.0). The molecular weight of these samples was evaluated by using the calibration curve constructed from the data for seven reference

proteins: bovine serum albumin (66 kDa), ovalbumin (45 kDa), porcine stomach pepsin (34.7 kDa), bovine erythrocytes carbonic anhydrase (29 kDa), bovine pancreas trypsinogen (24 kDa), horse heart cytochrome C (12.4 kDa), and bovine lung aprotinin (6.5 kDa).

SDS-polyacrylamide gel electrophoresis (SDS-PAGE) The blue protein solution was also subjected to SDS-polyacrylamide gel electrophoresis (SDS-PAGE) according to Laemmli (Laemmli 1970) , by using Ato AE-6200 slab-electrophoresis apparatus. Gel concentration of 20 % was found to be suitable for this sample system. The molecular weights of appeared bands were evaluated by using the calibration curve made from the data of the reference proteins: bovine serum albumin (66 kDa), ovalbumin (45 kDa), porcine stomach pepsin (34.7 kDa), bovine erythrocytes carbonic anhydrase (29 kDa), bovine pancreas trypsinogen (24 kDa), hen egg white lysozyme (14.3 kDa), horse heart cytochrome C (12.4 kDa), and bovine lung aprotinin (6.5 kDa).

Matrix-assisted laser desorption/ionization time-of- flight mass spectrometry (MALDI TOF Mass) Matrix-assisted laser desorption/ionization time-of- flight mass spectrometry was carried out with a AppliedBiosystems Voyager DE-Pro MALDI-TOF Mass Spectrometer in the linear mode at 20-kV accelerating voltage. The spectrum was obtained by an average over 128 laser shots. The spectrum was calibrated using instrumental calibration, based on the parameters determined from analysis of horse heart muscle apomyoblobin (+1, 16952 and +1, 33904).

An aliquot of freeze-dried sample of the blue protein was dissolved in 50μl water. This sample solution was mixed with the matrix solution (10 mg/ml sinapinic acid in 0.1 % TFA in water/acetonitrile=2/1) at a ratio of 1:9. A 1 μL of the sample solution was applied to the target and followed by drying at room temperature and atmospheric pressure.

ICP-AES measurement The amounts of iron and aluminum in the fractions of the anion exchange chromatography for the blue protein in the shell and for the colorless protein in the mantle were measured by inductively coupled plasma-atomic emission spectrometry (ICP-AES method) using a Varian Liberty Series II, according to standard addition method. The detection wavelengths of emission from iron and aluminum were 259.940 nm and 396.152 nm, respectively. The detection limits for iron and aluminum were 0.3×10^{-6} moldm^{-3} and 1.0×10^{-6} moldm^{-3}, respectively.

Attempt to extract chromophore It is well known that heme and porphyrins are one of the typical chromophores in many biological systems. In order to examine these possibilities, we attempted to separate heme or porphyrine from the protein and extract into organic solvent. The following six kinds of treatment of the sample were performed. 1) Hydrochloric acid-acetone treatment (Yamaguchi and Ogata 1978); a 1 ml of the blue protein solution was added dropwise to 10 volume of HCl-acetone (1:400 V/V) under vigorous stirring at -10 ℃, 3 ml of concentrated hydrochloric acid was added, then the acetone moiety was evaporated in a vacuum desiccator under reduced pressure for 3 days, the sample was dried in a vacuum desiccator in the presence of diphosphorus pentoxide, a 5% H_2SO_4-methanol was added to the residue for esterification, finally the resulting substance was extracted into chloroform after washing with water. 2) Hydrochloric acid-methanol treatment (Low and Bada 1974); 1 ml of the blue protein solution was added dropwise to 3 ml of 10 % HCl-methanol under stirring, boiled in a hot water bath for 20 min, after cooling with ice water, the sample was dried in a vacuum desiccator in the presence of diphosphorus pentoxide, a 5% H_2SO_4-methanol was added to the residue for esterification, finally the resulting substance was extracted into chloroform after washing with water. 3) Potassium hydroxide-methanol treatment (Yamaguchi and Matsuura 1969); 1 ml of the blue protein solution was added dropwise to 2 ml of 5 % KOH-methanol under stirring, boiled in a hot water bath for 5 min, after cooling with ice water, 0.4 ml of acetic acid was added to neutralize the solution, finally the resulting substance was extracted into 1 ml of chloroform. 4) Acetic acid-silver nitrate treatment (Paul 1950); 2 ml of the blue protein solution was added in the dark to the mixed solution between 0.5 ml of 1 moldm^{-3} silver nitrate aqueous solution and 2.5 ml of glacial acetic acid, kept in the dark at 80 ℃ for 120 min using a constant temperature bath, finally 1 ml of chloroform was added to the solution for extraction of chromophore. 5) Performic acid treatment (Omenn et al. 1970); 1 ml of the blue protein solution was added dropwise to the mixture between 5 ml of

formic acid and 1 ml of methanol below 0 ℃, 3 ml of performic acid was added and the solution was allowed to stand for 2 hours, 5 ml of the resultant solution was diluted with 15 ml of cold water and finally 1 ml of chloroform was added for extraction of chromophore. 6) HOAc-sulfenyl chloride treatment (Fontana et al. 1973); 1 ml of the blue protein solution was added to 1 ml of 50 % acetic acid under stirring, 1 ml of the solution between 0.05 g 2-nitrobenzene sulfenyl chloride and 1 ml acetic acid was added and stirred for 10 min, the solution was diluted with 5 ml of water, finally 1 ml of chloroform was added for extraction of chromophore. After each of these treatments, it was examined whether some colored substance could be extracted into chloroform phase. Concerning the former three treatments (hydrochloric acid-acetone treatment, hydrochloric acid-methanol treatment, and potassium hydroxide-methanol treatment), the same treatment was performed using the protein having no chromophore (hen egg albumin), and it was assured whether or not chloroform phase coloring was a result of extraction of some chromophore.

In order to examine whether the blue protein is caroteoprotein or not, we attempted to separate the chromophore by acetone-ether method (Renstrom et al. 1982, Zagalsky 1985). A 6 ml of acetone was added to 5 ml of the blue protein solution, then 10 ml of diethyl ether was added and mixed. It was examined whether some colored substance could be extracted into the ether phase.

Examination of labile sulfide To examine the possibility that the blue protein is an iron-sulfur protein, it was examined whether labile sulfide was present by transforming into methylene blue in the presence of N, N-dimethyl-p-phenylenediamine and iron chloride (Fogo and Popowsky 1949a, Fogo and Popowsky 1949b, Brumby et al. 1965, Massey et al. 1969). A 2 ml of 1% zinc acetate and 0.1 ml of 12% sodium hydroxide were added to a 0.3 ml of the blue protein solution and mixed slowly. A 0.5 ml of 0.1% N, N-dimethyl-p-phenylenediamine in 5 moldm^{-3} hydrochloric acid and 0.1 ml of 0.023mol dm^{-3} iron(III) chloride in 1.2 moldm^{-3} hydrochloric acid were quickly added to the solution, and mixed vigorously for 30 min every 5 minutes. After centrifugation, the absorbance of the supernatant was measured at 670 nm.

ESR measurement In order to investigate the state of iron, the ESR spectra of the blue protein and the sample in the presence of the reducing agent and KCN were measured using the ESR spectrometer JOEL JES-RE2X and compared. The measurement conditions were sample temperature of 77 K (liquid nitrogen), H = 250 mT, and ν = 9.080 GHz.

Circular dichroism measurement and analysis In order to evaluate the secondary-structure contents of the blue protein, circular dichroism (CD) spectrum was measured with a Jasco J-600 spectropolarimeter. The relative proportions of secondary structures (α-helix, β-sheet, and random coil) were calculated by a least-square fit analysis using the reference spectra of those secondary structures (Chen et al. 1974). At any wave length, CD of the blue protein may be expressed by the reference data as

$$[\theta] = f_{\mathrm{H}}[\theta]_{\mathrm{H}} + f_{\beta}[\theta]_{\beta} + f_{\mathrm{R}}[\theta]_{\mathrm{R}} \qquad (1)$$

where $[\theta]_{\mathrm{H}}$, $[\theta]_{\beta}$ and $[\theta]_{\mathrm{R}}$ are CD of α-helix, β-sheet and random coil forms, respectively, and f_{H}, f_{β}, and f_{R} are the fractions of those forms. Under the condition that the sum of the fractions equal to unity, the fractions were determined so as to minimize sum of square of the difference between observed CD and $[\theta]$ of eq. (1) over the observed wave lengths.

3. RESULTS and DISCUSSION

Anion exchange chromatography

Figure 2 shows the elution profile of anion-exchange chromatography of the blue protein. It can be seen that there are two blue components (A: around tube number 47 and B: around tube number 57). The fact that A was eluted faster than B suggests that B is more negatively charged than A at pH 7.0. The two blue components with absorbance 0.2 or higher were subjected to subsequent analyses. In the case of the sample extracted from the mantle, the colorless component (C) was observed around tube number 36 in a large amount in addition to the component A (see Fig. 7B). The rapid elution of this C component indicates that the anionic charge of the C component is lesser than those of A and B complonents.

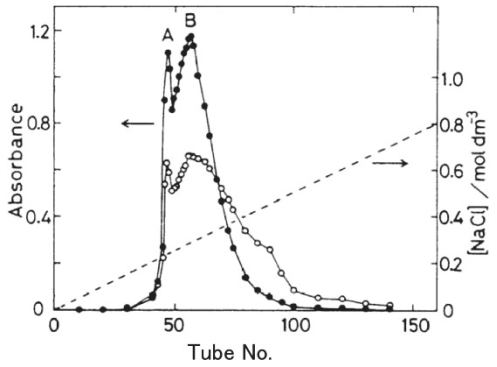

Figure 2. Anion exchange chromatography of the blue protein of *Ruditapes philippinarum* with a DEAE-TOYOPEARL 650 column (26.4 mm×450 mm) in 0.01 moldm^{-3} phosphate buffer (pH=7.0) under a linear gradient of NaCl (0—1 moldm^{-3}). Flow rate is 1.25 ml/min, and 10 ml was collected in one tube. The absorbance was measured at 278 nm (○) and 627 nm (●).

From the values of the absorbance of A and B components at 627 nm and the mass obtained by drying the sample, the average molecular extinction coefficient at 627 nm was estimated to be about $\varepsilon_{627}=5\times10^4$ mol^{-1} cm^{-1} assuming a molecular weight of 10 kDa (see the results of molecular weight measurements).

Amino-acid composition of the blue protein and the mantle protein.

Table 1 shows the Amino acid composition of the blue protein and of the protein in the mantle. Although cys-cys is contained in both samples, it may actually be contained in a larger amount because it is usually easily decomposed by hydrochloric acid hydrolysis.

It can be seen from this table that the amino acid compositions of these two samples are homologous to each other. These proteins are rich in acidic amino acids such as aspartic acid and glutamic acid, and their total accounts for nearly 30% of the total amino acids. Based on the amino acid composition, the isoelectric point of the blue protein was estimated as *pI*=3.96 by using the Protein Identification and Analysis Tools on the ExPASy Server. This shows that the blue protein and the mantle protein are acidic proteins, showing the characteristics common to the matrix of marine shells (Song et al. 2019).

Evaluation of secondary structure from CD spectrum

Figure 3 shows CD spectrum of the blue protein. The CD spectrum of the blue protein presented two negative peaks at 208 and 222 nm which is typical for the presence of α-helix elements in a protein. The relative proportions of secondary structures were estimated as the content of α-helix structure=28.6 (±1.0) %, the content of β-sheet structure=20.1 (±1.0) %, and the content of random coil structure=51.3 (±1.0) %.

Table 1. Amino acid composition of the blue protein and of the protein in the mantle.

amino acids	Mole composition / %	
	the blue protein	the mantle protein
Asp	13.75	13.61
Thr	5.23	7.07
Ser	5.08	6.84
Glu	12.37	11.74
Pro	7.86	6.26
Gly	11.02	10.24
Ala	8.22	7.83
Cys-Cys	1.36	2.25
Val	5.47	4.76
Met	2.17	1.53
Ilu	5.13	2.8
Leu	5.47	6.23
Tyr	4.62	3.02
Phe	3.07	3.98
Lys	3.63	6.29
His	1.28	1.35
Arg	4.27	4.22

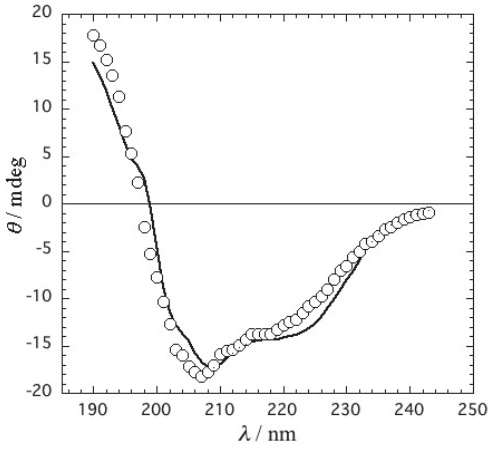

Figure 3. CD spectrum of the blue protein. Circles show the experimental data. The solid curve shows the calculated spectrum from the parameters evaluated by the least-square fit analysis using the reference spectra of α-hellix, β-sheet, and random coil structures (see text).

Molecular weights.

Figure 4 shows the elution profile of the blue protein measured by the size-exclusion chromatography using a TSK3000SWxL column. This figure shows that the blue component was eluted at 10.21 min, while another colorless component with a low molecular weight was eluted at 11.08 min. The molecular weights of these components have been estimated as 40.7±1.5 kDa for the blue component and 25.7±1.5 kDa for the colorless component, by using the calibration curve constructed from the data for the seven reference proteins.

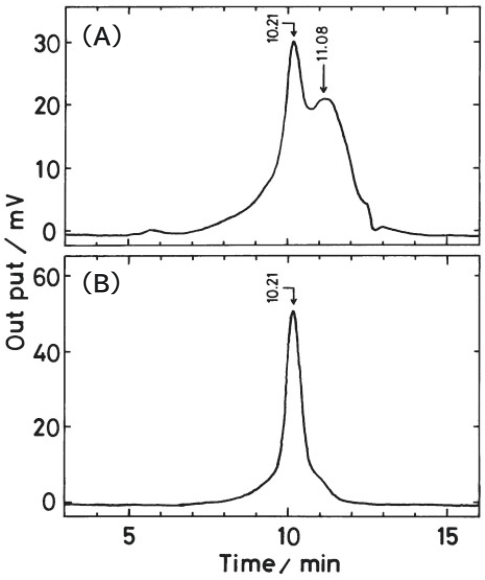

Figure 4. Size-exclusion chromatography of the blue protein using a TSK3000SWxL column (7.8 mm×300 mm) in 0.1 moldm^{-3} phosphate buffer (pH=7.0). Flow rate is 1 ml/min. Light absorption was observed at (A) 276 nm and (B) 627 nm.

Figure 5 shows SDS-PAGE patterns of the blue protein and the reference proteins.

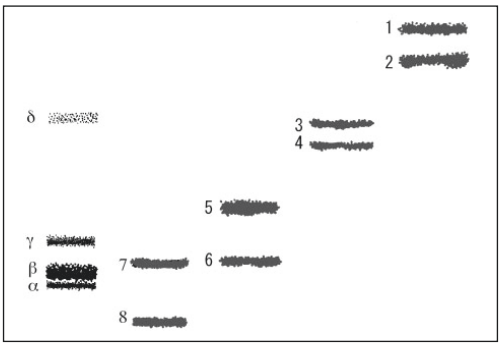

Figure 5. SDS-polyacrylamide gel electrophoresis of the blue protein with a 20 % gel concentration. The numbers show the reference proteins; 1: bovine serum albumin, 2: ovalbumin, 3: porcine stomach pepsin, 4: bovine erythrocytes carbonic anhydrase, 5: bovine pancreas trypsinogen, 6: hen egg-white lysozyme, 7: horse heart cytochrome C, and 8: bovine lung aprotinin.

This figure shows that the blue protein is composed of four protein bands (α, β, γ, and δ). The molecular weights of these bands have been estimated as α=9.9±1.2 kDa, β=10.4±1.3 kDa, γ=13.1±1.6 kDa, δ=28±3 kDa.

Figure 6 shows the MALDI TOF Mass spectrum of the blue protein.

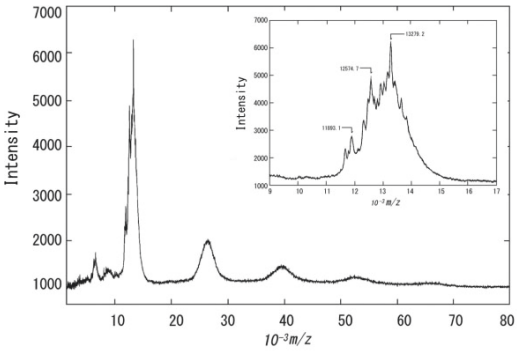

Figure 6. MALDI TOF Mass spectrum of the blue protein in the shell-surface pattern of *Ruditapes philippinarum*. The insertion shows an enlarged view of the region from 9000 to 17000 in *m/z* value.

We can see from this figure that multiple peaks are lined up at an equal interval (12900 in *m/z*). We can see also from the insertion that there are three peaks in the low *m/z* region around 13000 (*m/z*=11900, 12600 and 13300). The above-mentioned sequence of species with evenly spaced molecular weights can be thought as the alinement of from monomer to pentamer of the species present near *m/z*=13000.

Table 2 summarizes the molecular weights of the blue protein in the shell-surface pattern of *Ruditapes philippinarum* obtained from the three methods of analysis. Among these methods of analysis, the experimental condition for the SEC measurement is closest to the native condition. From the SEC measurement, it was found that molecular weight of the blue components is more than 30 kDa. On the other hand, SDS-PAGE and MALDI TOF Mass measurements show multiple components with molecular weights of around 10 kDa. Taking experimental errors into account, these low molecular weight components around 10 kDa are considered to be the same species. From these

Table 2. Molecular weights of the blue protein in the Shell-surface pattern of *Ruditapes philippinarum* obtained from three methods of analysis. In MALDI TOF Mass, the value of z is assumed to be +1.

Method	*Molecular weight* / kDa					
SDS-PAGE	9.9±1.2	10.4±1.3	13.1±1.6	28.0±3.0		
SEC				25.7±1.5	40.7 ± 1.5	
MALDI TOF Mass	11.9	12.6	13.2	25.9	38.8	51.7

observations, it is considered that the blue protein is formed as trimer or tetramer of the monomer species having molecular weights of around 10 kDa.

Furthermore, the components A and B separated by the anion exchange chromatography correspond to the trimer and tetramer of these low molecular weight components, respectively. This is because, the tetramer having larger anionic charges than the trimer must be eluted later than the trimer in the anion exchange chromatography. The species having molecular weight around 26 kDa in Table 2 can be thought as dimer species.

Amount of Fe and Al relative to the amount of protein

Figure 7 shows the comparison between elution profiles of the blue protein and the protein in the mantle obtained by the anion exchange chromatography measured by UV-VIS absorption and by ICP-AES. The shell sample used for these measurements is different from that in Fig.2. Comparing between Fig.7(A) and Fig.2 shows that the elution profiles are slightly different to each other. In particular, components with a small number of charges (low molecular weight) that do not have blue color can be seen in the fractions before tube No. 40. This component is considered to be monomer or dimer of the proteins of around 10 kDa. From Fig.7(B), we can see that the low molecular-weight component was also observed in the elution profile for the mantle sample.

Elution profile of Fe for the blue protein appears to follow the elution curve of the trimers and above (Fig.7(A)). On the other hand, Al was present in very small quantities near the detection limit. Furthermore, the elution profiles of Fe and Al for the mantle protein indicate that the mantle protein hardly binds Fe and Al.

From the value of absorbance at around the elution peak for 627 nm (Absorbance=4), the value of 5-fold diluted Fe concentration at the peak ([Fe]=4×10^{-6} moldm^{-3}) and the value of molecular extinction coefficient at 627 nm ($\varepsilon_{627}=5\times10^{4}$ mol^{-1}cm^{-1}), the number of iron atom bound per monomer molecule having a molecular weight of 10 kDa was calculated to be about 0.25. This indicates that one Fe atom is bound per tetramer of the protein having molecular weight of 10 kDa.

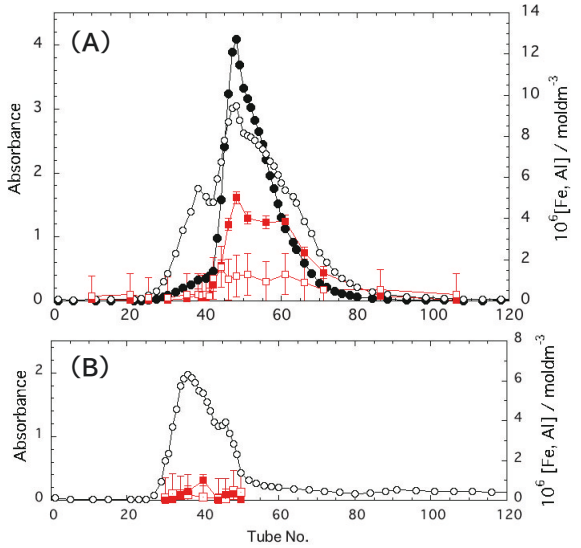

Figure 7. Comparison between elution profiles of the blue protein (A) and the protein in the mantle (B) obtained by the anion exchange chromatography measured by UV-VIS absorption and by ICP-AES. The experimental conditions are the same as those in Fig. 2. Filled black circle shows absorbance at 627 nm, and open circle shows that at 278 nm. Filled red square and open square show concentrations of Fe and Al, respectively. The concentrations show the values diluted 5-fold.

A possible mechanism of formation of the shell surface pattern color

From the above observation, the formation mechanism

of the blue protein can be considered as follows. In the mantle, the protein exists in the form of monomer or dimer which does not bind Fe and has no absorption band around 627nm. In the shell formation, during the matrix formation of the outermost layer (periostracum) of the shell, aggregates in which one iron atom is bound to trimer or tetramer of the proteins of about 10 kDa are formed. These aggregates are colored blue. The distribution of these aggregates along the edge of the shell is not always uniform but mottled by a neural-net mechanism (Saleuddin ASM 1979, Saleuddin and Kunigelis 1984, Boettiger et al. 2009), resulting in the formation of shell patterns as the shell grows. Here, if ferric ions are required for the formation of the aggregates, it is possible to hypothesize that the secretion of ferric ions and complexation with the protein governs the formation of shell pattern.

The blue-colored periostracum of the shell must have a certain thickness. When this layer is formed and exposed to seawater, the outside of this layer might be more or less denatured and changes color from blue to brown under the influence of the surrounding chemical environment. As a result, the five colors of the raw shell pattern are produced by superimposing the brown color of the denatured outer layer and the blue color of the undenatured inner layer. This mechanism can well interpret the fact mentioned in introduction that the brown area of the outer layer and the blue areas of the inner layer overlap exactly.

Effect of agents on absorption spectrum and association state

Figure 8 shows the effect of reducing agents (sodium hydrosulfite, hydroxylamine hydrochloride) and KCN on the absorption spectrum of the blue protein. By addition of these reagents, the absorption spectrum shifted to the lower wavelength side, and the blue color changed to from redish purple to pink. In the case of hydroxylamine hydrochloride, bleaching occurred following the initial change with an isosbestic point near 570 nm. In the case of 2-mercaptoethanol addition, bleaching also occurred with a slow change in date order following the change in hour order.

Figure 9 shows the effect of hydroxylamine hydrochloride on the elution profile of size-exclusion chromatography. Addition of hydroxylamine hydrochloride or 2-mercaptoethanol reduced the band with a molecular weight of around 40 kDa, instead the low molecular-weight bands of 23 kDa or less appeared (compare with Fig.4). These low molecular-weight bands showed no light absorption in the 620nm region. In conclusion, the addition of these reducing agents causes dissociation of the trimer and/or tetramer and decolorization. On the other hand, the absorption spectrum after adding KCN was relatively stable for a long time.

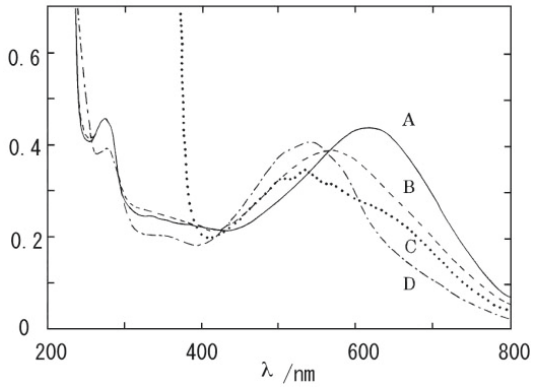

Figure 8. Effect of reducing agents and KCN on the absorption spectrum of the blue protein; A: native protein, B: in the presence of 0.45 moldm^{-3} NH_4OH・HCl , C: 0.45 moldm^{-3} $Na_2S_2O_4$, and D: 0.45 moldm^{-3} KCN.

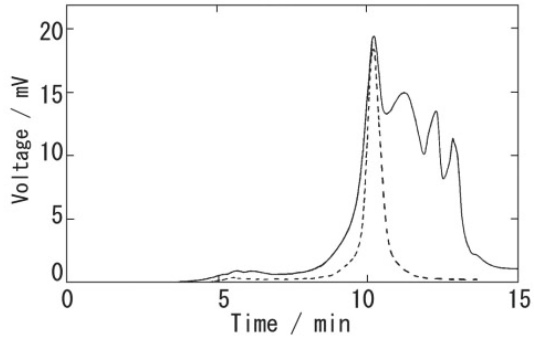

Figure 9 Size-exclusion chromatography of the blue protein in the presence of hydroxylamine hydrochloride, with a TSK3000SWxL column (7.8 mm×300 mm) in 0.1 moldm^{-3} phosphate buffer (pH=7.0). Solid curve shows the absorbance observed at 278nm, and the broken curve shows that at 627 nm.

Chromophore

Concerning the possibility of heme and porohyrins as the chromophore, no colored substance that could be attributable to them was extracted into the chloroform phase by any of the performed treatments. In many cases of these treatments, brown colored precipitate was observed at the boundary between aqueous phase and chloroform phase, or, in the case of HOAc-sulfenyl chloride

treatment, brown or green colored precipitate was observed in the chloroform phase. These observations indicate that the chromophore did not leave the protein moiety by these treatments and precipitated with the denatured protein. This result suggests that the blue protein is unlikely to be a heme protein or a biliprotein, otherwise, the chromophore is in a bound state that does not break off from protein moiety by these treatments. Concerning the possibility of carotenoprotein, no colored substance was extracted into the ether phase by the performed treatment. This suggests that the possibility that the blue protein is a carotenoprotein is low. In conclusion, the possible structure of the chromophore could not be extracted.

Existence states of iron atom

Figure 10 shows the ESR spectra of the native blue protein and in the presence of KCN and $Na_2S_2O_4$. Concerning the native protein, two absorption bands (g=4.25 and g=2.06) can be seen.

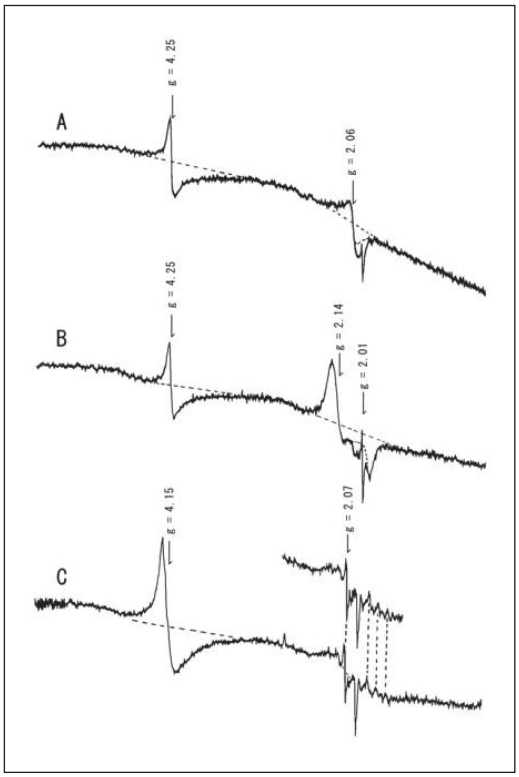

Figure 10. ESR spectra of the blue protein; A: native protein, B: in the presence of KCN, C: in the presence of $Na_2S_2O_4$.

Of these, the band at g=4.25 is a typical signal of ferric iron in a weak ligand field (Ohya & Yamauchi, 1989). More specifically, 1) a high-spin (5/2) 6-coordination complex in which a ligand that brings a low-symmetry ligand field to porphyrin, 2) a low-symmetry 6-coordination complex containing N, O, and in some cases S, and 3) a 6-coordinated complex of intermediate spin (3/2). A rubredoxin-like structure in which iron ions form a mononuclear tetrahedron with the sulfur atoms of four cysteine residues might be also a possible structure (Bachmayer et al. 1967). Since the presence of inorganic sulfur was not found as the result of searching for labile sulfide, the possibility of poly-nuclear iron-sulfur protein is low. The band at g=2.06 is in the region where a low spin (1/2) ferric iron signal appears in a strong ligand field.

While the band at g=4.25 was not affected by KCN addition, the band at g=2.06 disappeared instead the bands at g=2.14 and g=2.01 appeared. From these observations, the following things can be considered. There are two types of ferric iron. Concerning the species giving the absorption band at g=4.25, coordinated ligands cannot be replaced by CN^-. On the other hand, for the species giving the absorption band at g=2.06, at least one of the coordinated ligands is replaced by CN^- to give the bands at g=2.14 and g=2.01.

When the reducing agent $Na_2S_2O_4$ was added, the band at g=2.06 disappeared, instead the two bands appeared: one is the band at g=2.07 that seems to be a radical and the other is the band at lower g values that seems to be derived from Mn^{2+}. On the other hand, the intensity of the band at g=4.25 became large and the g value shifted to 4.15, suggesting multiple bands overlapping. From the above observations, the effect of $Na_2S_2O_4$ can be considered as follows. The species giving the band g=2.06 was reduced by $Na_2S_2O_4$ and disappeared. The appearance of the signal based on Mn^{2+} suggests that there is a spin coupling between Fe^{3+} and Mn^{2+} in the native state, but the coupling was broken by the reduction of Fe^{3+}. Species that give the band g=4.25 was not reduced by $Na_2S_2O_4$, but was somehow affected by this reducing agent.

4. SUMMARY

Characterization of the blue protein in the shell pattern of Japanese littleneck clam (*Ruditapes philippinarum*) was performed by purification using anion-exchange chromatography, amino acid analysis of the protein and the mantle protein, molecular weight measurements using size exclusion chromatography (SEC), SDS-polyacrylamide gel electrophoresis (SDS-PAGE) and matrix-assisted laser desorption/ionization time-of-flight

mass spectrometry (MALDI TOF Mass), quantification of ferric ions and aluminum ions using inductively coupled plasma-atomic emission spectrometry (ICP-AES), examination of the existence state of iron ions by electron spin resonance (ESR) measurement, estimating secondary structure by CD measurement, etc. Blue colored two components were found by the anion exchange chromatography. From the amino acid composition, it was found that the blue colored shell protein and the colorless mantle protein were homologous to each other; they are acidic proteins rich in aspartic acid and glutamic acid and that the isoelectric point of the blue protein was estimated as *pI*=3.96. The secondary structure of the blue protein was estimated from CD spectrum as α-helix (28.6%), β-sheet (20.1%), and random coil (51.3%). From combination of the results of molecular weight measurements and quantification of ferric ions, it was found that the blue protein is formed as trimer or tetramer from the monomer proteins of about 10 kDa by complexing with ferric ion. From light absorption and ESR spectra in the absence and presence of reducing agents and KCN, it was found that there are two kinds of ferric ion existing states and that reducing agents decompose the blue colored trimer or tetramer into dimer or smaller units accompanying decolorization. Elucidation of the structure of the chromophore, which is the cause of blue color, will be future challenges.

ACKNOWLEDGMENTS

The authors wish to express thanks to Dr. Yoshiko Murakami of Yamaguchi University for ICP-AES measurements; Dr. Kunio Takeda for CD measurements; Dr. Naohisa Kure for amino acid analysis; Dr. Kouto Migita for his help on the ESR measurements; UBE Scientific Analysis Laboratory, Inc. for amino acid analysis and MALDI TOF Mass measurements.

REFERENCES

Affenzeller S, Wolkenstein K, Frauendorf H, Jackson DJ (2019) Eumelanin and pheomelanin pigmentation in mollusc shells may be less common than expected: insights from mass spectrometry. *Front Zool* **16**: 47 https://doi.org/10.1186/s12983-019-0346-5.

Bachmayer H, Piette LH, Yasunobu KT, Whiteley HR (1967) The binding site of iron in rubredoxin from micrococcus aerogenes. *Biochemistry*, **57**, 122-127.

Bannister WH, Bannister JV, Micallef H (1970) A soluble pigment-protein complex from the shell of Monodonta turbinata. *Comp Biochem Physiol* **35**, 237-243.

Barnard W, De Waal D (2006) Raman investigation of pigmentary molecules in the molluscan biogenic matrix. *Journal of Raman Spectroscopy* **37**, 342–352.

Belcher AM, Wu XH, Christensen RJ, Hansma PK, Stucky GD and Morse DE (1996) Control of crystal phase switching and orientation by soluble mollusc-shell proteins. *Nature* **381**, 56–58.

Benedikt E, Albert Gossauer A, Kost H-P, Miki W, and Yamaguchi K (1988) Biliverdin IXδ and neobiliverdin IXδ, isolated from the ovaries of the marine snail, *Turbo cornutus*. *Eur J Biochem*, **175**, 643-648.

Boettiger A, Ermentrout B, Oster G (2009) The neural origins of shell structure and pattern in aquatic mollusks. *PNAS* **106**, 6837-6842.

Bonnard M, Cantel S, Boury B, Parrot I (2020) Chemical evidence of rare porphyrins in purple shells of Crassostrea gigas oyster. *Scientific Reports* **10**, 12150.

Brumby PE, Miller RW, Massey V (1965) The content and possible catalytic significance of labile sulfide in some metalloflavoproteins. *J Biol Chem*, **240**, 2222-2228.

Chen YH, Yang JT, Chau KH (1974) Determination of the helix and β form of proteins in aqueous solution by circular dichroism. *Biochemistry*, **13**, 3350-3359.

Cianci M, Rizkallah PJ, Olczak A, Raftery J, Chayen NE, Zagalsky PF, Helliwell JR (2002) The molecular basis of the coloration mechanism in lobster shell: β-Crustacyanin at 3.2-Å resolution. *Proc Natl Acad Sci USA*, **99**, 9795–9800.

Dubey S, Roulin A (2014) Evolutionary and biomedical consequences of internal melanins. *Pigment Cell Melanoma Res* **27**, 327–338.

Falini G, Albeck S, Weiner S and Addadi L (1996) Control of aragonite or calcite polymorphism by mollusk shell macromolecules. *Science* **271**, 67-69.

Fogo JK, Popowsky M (1949a) Spectrophotometric determination of hydrogen sulfide. Methylene blue method. *Anal Chem*, **21**, 732-734.

Fogo JK, Popowsky M (1949b) Conversion of sulfur compounds to hydrogen sulfide in air, fuel gas, or mixtures. *Anal Chem*, **21**, 734-737.

Fontana A, Veronese FM, Boccu E (1973) Reaction of sulfenyl halides with cytochrome c. A novel method for heme cleavage. *FEBS Lett* **32**, 135-138.

Fowler DR, Meinhardt H, Prusinkiewicz P (1992)

Modeling seashells. *Comput Graphics* **26**, 379–387.

Gasteiger E, Gattiker A, Hoogland C, Ivanyi I, Appel RD, Bairoch A (2003) ExPASy: the proteomics server for in-depth protein knowledge and analysis. *Nucleic Acids Res* **31**, 3784-3788.

Hedegaard C, Bardeau J-F, Chateigner D (2006) Molluscan shell pigments: an in-situ resonance Raman study. *J Mollusc Stud* **72**, 157-162.

Jiang K, Jiang L, Nie H, Huo Z, Yan X (2020) Molecular cloning and expression analysis of tyrosinases (tyr) in four shell-color strains of Manila clam *Ruditapes philippinarum. PeerJ* **8**: e8641 https://doi.org/10.7717/peerj.8641.

Kobayashi I (1996) Function and phylogenetic evolution of hard tissues: Function and biological information of molluscan shell. In: Wada K, Kobayashi I (eds) *Biomineralization and hard tissue of marine organisms*. Tokai University Press, Tokyo, pp205-218.

Kochiyama Y, Yamaguchi K, Hashimoto K, Matsuura F (1966) Studies on a blue-green serum pigment of eel (II). Identification of prosthetic group. *Bull Japan Soc Sci Fish*, **32**, 873-880.

Kondrachuk AV, Wiederhold ML (2001) Model of statoconia accumulation in gravireceptors of mollusks. *J Gravit Physiol* **8**, 109-110.

Kondrachuk AV, Boyle RD (2006) Feedback hypothesis and the effects of altered gravity on formation and function of gravireceptors of mollusks and fish. *Arch Ital Biol* **144**, 75-87.

Laemmli UK (1970) Cleavage of structural proteins during the assembly of the head of bacteriophage T4. *Nature*, **227**, 680-685.

Low PS, Bada JL (1974) Bile pigments in the blood serum of fish from the family Cottidae. *Com Biochem Physiol* **47**A, 411-418.

Massey V, Brumby PE, Komai H (1969) Studies on milk xanthine oxidase. *J Biol Chem* **244**, 1682-1691.

Meinhardt H (1984) Models for positional signaling, the threefold subdivision of segments and the pigmentation pattern of molluscs. *J Embryol Exp Morphol* **83**, 289-311.

Meinhardt H, Klingler M (1987) A model for pattern formation on shells of molluscs. *J Theor Biol* **126**, 63-89.

Meinhardt H, Prusinkiewicz P, Fowler D (2003) The algorithmic beauty of sea shells. (Springer, New York), 3rd Ed.

Milicua JCG, Barandiaran A, Macarulla JM, Garate, AM, Gomez R. (1985) Structural characteristics of the carotenoids binding to the blue carotenoprotein from Procambarus clarkii. *Experientia* **41**, 1485–1486.

Miyashita T, Takagi R (2011) Tyrosinase causes the blue shade of an abnormal pearl. *J Mollusc Stud* **77**, 312–314.

Murakami K, Tamura S (1995) A study on the shell pattern of Japanese littleneck clam (*Ruditapes philippinarum*) (I). *Chem Edu* **43**, 41-44. (in Japanese)

Murray JD (2003) Mathematical Biology (Springer, New York), 3rd Ed, pp 638–655.

Ohya H, Yamauchi J (1989) Electron spin resonance (Kodansha Ltd. Tokyo) pp 207–228. (in Japanese)

de Oliveira LN, de Oliveira VE, D'avila S, Edwards HG, de Oliveira LF (2013) Raman spectroscopy as a tool for polyunsaturated compound characterization in gastropod and limnic terrestrial shell specimens. *Spectrochim. Acta Part A: Molecular and Biomolecular Spectroscopy* **114**, 541–546.

Omenn GS, Ontjes DA, Anfinsen CB (1970) Immunochemistry of staphylococcal nuclease. I. Physical, enzymatic, and immunological studies of chemically modified derivatives. *Biochemistry*, **20**, 304-312.

Paul KG (1950) The splitting with silver salts of the cysteine-porphyrin bonds in cytochrome c. *Acta Chem Scand* **4**, 239-244.

Renstrom B, Ronneberg H, Borch G, Liaaen-Jensen S (1982) Animal carotenoids—27. Further studies on the carotenoproteins crustacyanin and ovoverdin. *Comp Biochem Physiol B* **71**, 249-252.

Saleuddin ASM (1979) Shell formation in molluscs with special reference to periostracum formation and shell regeneration. In *Pathways in Malacology*, Spoel S Van der, Bruggen AC Van, Lever J (eds) (Junk, The Hague), pp 47–81.

Saleuddin ASM, Kunigelis SC (1984) Neuroendocrine control mechanisms in shell formation. *Am Zool* **24**, 911–916.

Song X, Liu Z, Wang L, Song L (2019) Recent advances of shell matrix proteins and cellular orchestration in marine molluscan shell biomineralization. *Front Mar Sci* **6**:41. doi: 10.3389/fmars.2019.00041.

Speiser DI, DeMartini DG, Oakley TH (2014) The shell-eyes of the chiton Acanthopleura granulata (Mollusca, Polyplacophora) use pheomelanin as ascreening pigment. *J Nat Hist* **48**, 45–48.

Verdes A, Cho W, Hossain M, Brennan PLR, Hanley D, Grim T, Hauber ME, Holford M (2015) Nature's palette: characterization of shared pigments in colorful avian and mollusk shells. *PLOS ONE* **10**: e0143545.

Wade NM, Tollenaere A, Hall MR, Degnan BM (2009) Evolution of a novel carotenoid-binding protein responsible for crustacean shell color. *Mol Biol Evol* **26**, 1851–1864.

Williams ST, Ito S, Wakamatsu K, Goral T, Edwards NP, Wogelius RA, Henkel T, de Oliveira LFC, Maia LF, Strekopytov S, Jeffries T, Speiser DI, Marsden JT (2016) Identification of shell colour pigments in marine snails clanculus pharaonius and c. margaritarius (*Trochoidea; Gastropoda*). *PLOS ONE* **11**: e0156664

Williams ST (2017) Molluscan shell color. *Biol Rev* **92**, 1039–1058.

Yamaguchi K, Matsuura F (1969) A blue pigment from the muscle of a marine teleost, "Hirosa", *Cheilinus undulatus* Rüppell. *Bull Jpn Soc Sci Fish* **35**, 920-926.

Yamaguchi K, Ogata T (1978) Isolation and characterization of a biliprotein from the ovary of a turban shell, *Turbo cornutus. Bull Jpn Soc Sci Fish* **44**, 631-637.

Zagalsky PF (1985) Invertebrate carotenoproteins. *Methods Enzymol* **111**, 216-247.

Zhang G, Fang X, Guo X, Li L, Luo R, Xu F, Yang P, Zhang L, Wang X, Qi H, Xiong Z, Que H, Xie Y, Holland PW, Paps J et al. (2012) The oyster genome reveals stress adaptation and complexity of shell formation. *Nature* **490**, 49–54.